

Supporting Information for:  
“Birth of the Hydrated Electron via Charge-Transfer-to-Solvent  
Excitation of Aqueous Iodide”

Kevin Carter-Fenk,<sup>1,2,3\*</sup> Britta A. Johnson,<sup>1</sup> John M. Herbert,<sup>3†</sup>  
Gregory K. Schenter,<sup>1</sup> and Christopher J. Mundy<sup>1,5‡</sup>

<sup>1</sup>*Physical Science Division, Pacific Northwest National Laboratory,  
Richland, Washington 99352, USA*

<sup>2</sup>*Department of Chemistry, University of California,  
Berkeley, California 94720, USA*

<sup>3</sup>*Department of Chemistry & Biochemistry, The Ohio State University,  
Columbus, Ohio 43210, USA*

<sup>4</sup>*Department of Chemical Engineering, University of Washington,  
Seattle, Washington 98195, USA*

January 8, 2023

## S1 Procedure to Determine Local Potential Energy Surfaces

In Fig. 5b, we show two distinct electronic states corresponding to the ground state of  $I^-(aq)$  state and  $e^-(aq)$  state following excitation and solvent relaxation. The local potential energy surfaces were determined by analyzing fluctuations in the solvent’s electrostatic potential along the corresponding *ab initio* molecular dynamics trajectory, as follows. We computed an approximate electrostatic potentials along each trajectory by replacing water molecules from the *ab initio* trajectory with atomic point charges taken from the SPC/E water model.<sup>1</sup> Fluctuations in this potential, evaluated at the coordinates of the solute of interest, provide an easy means to construct a solvent coordinate. For the ground state of  $I^-(aq)$ , this electrostatic potential was evaluated at the location of the iodine atom, for 106,997 configurations along a trajectory of  $\approx 50$  ps in length. These data were then binned into 40 intervals, with a spacing of  $\delta = 6.1 \times 10^{-3}$  a.u.. For the the solvated electron, the electrostatic potential was evaluated at the Wannier center representing the SOMO, for 1,108 configurations along a trajectory of  $\approx 14$  ps. In either case, the resulting histogram was fit to a Gaussian function,

$$f(x) = ae^{-(x-b)^2/2c^2} . \quad (S1)$$

---

\*carter-fenk@berkeley.edu

†herbert@chemistry.ohio-state.edu

‡chris.mundy@pnnl.gov

The fit then affords an electronic surface

$$V(x) = -k_{\text{B}}T \ln f(x), \tag{S2}$$

where  $k_{\text{B}}$  is the Boltzmann constant and  $T$  is the temperature.

The value of the electrostatic potential captures the extensive reorganization and rearrangement that the water molecules undergo during creation of a solvated electron, though this construction of a solvent coordinate is certainly not unique. Our approximation is to use the thermal fluctuation in the solvent potential to determine the curvature of a Gaussian fit, similar to earlier approaches in the literature in which umbrella sampling is used to determine the entire free energy surface.<sup>2,3</sup> We attribute no real meaning to the potential values; rather, they serve a descriptor for solvent reorganization.

The offset energy from the  $\text{I}^{-}(\text{aq})$  ground state to the  $\text{I}^{-*}/\text{CTTS}$  state was determined to be around 5.5 eV due to the initial ROKS excitation energy, as seen from Fig. 1 at  $t = 0$ . For the  $\text{I}^{-}(\text{aq})$  ground state, we ran a short trajectory of 1.8 ps using same level of theory that was used to calculate the much longer 14 ps trajectory for  $e^{-}(\text{aq})$ . The consistent level of theory allows us to make a direct comparison between the energies, and this comparison is shown in Fig. S1. [The zero of energy in Fig. S1 corresponds to the average energy energy of the  $\text{I}^{-}(\text{aq})$  ground state.] From Fig. S1, we determined the offset energy from the  $\text{I}^{-}(\text{aq})$  ground state to the  $e^{-}(\text{aq})$  state to be around 4 eV. However, our conclusions should not depend on the precise value of this offset, especially given the magnitude of the solvent reorganization (see Fig. 1). The local potential surfaces in Fig. 5b will be in the inverted regime for any energy offset within the statistical error bars of our results.

## S2 Additional Data

We have reproduced the formation of  $e^{-}(\text{aq})$  from ground-state  $\text{I}^{-}(\text{aq})$  simulations using the BLYP+D2, revPBE+D3, and PBEh(40)-rVV10 functionals for the ground-state part of the simulation. However, PBEh(40)-rVV10 yields an overstructured picture of  $\text{I}^{-}(\text{aq})$  hydration, and because of the microstate dependence of the initial CTTS state that is discussed in the main text, we use the simulation data from BLYP+D2 to represent the ground-state structure as this functional is known to reproduce the experimental hydration structure around  $\text{I}^{-}(\text{aq})$ .<sup>4-6</sup>

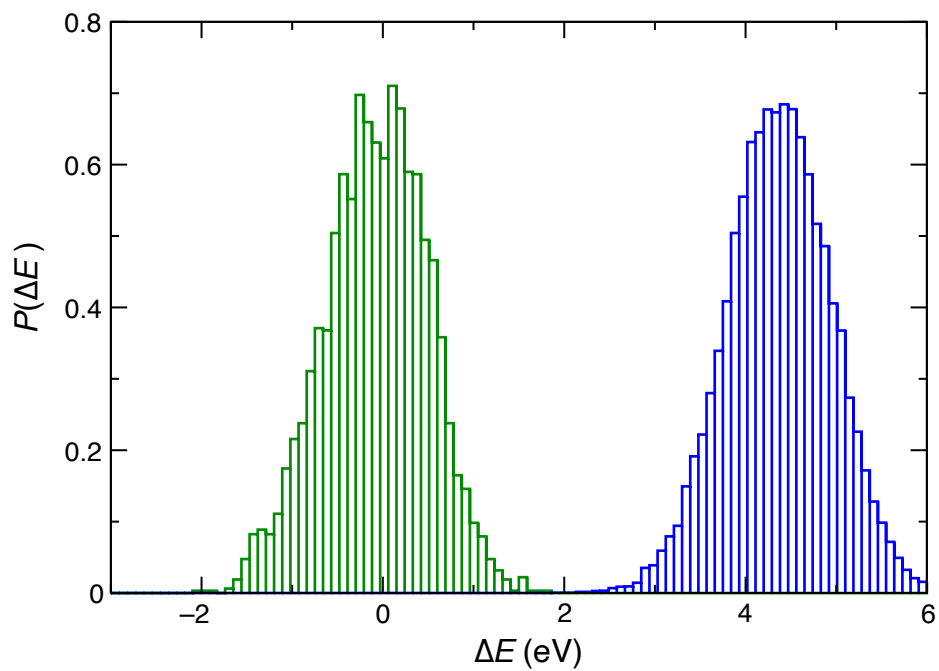


Figure S1: Binned energies from trajectories for  $\text{I}^-(\text{aq})$  and  $e^-(\text{aq})$ , in green and blue, respectively, at the level of theory used to describe  $e^-(\text{aq})$  as detailed in the text. The energy difference  $\Delta E$  between the two peaks, referenced to the average energy of  $\text{I}^-(\text{aq})$ , is used to determine the energy offsets between the local electronic surfaces in Fig. 5.

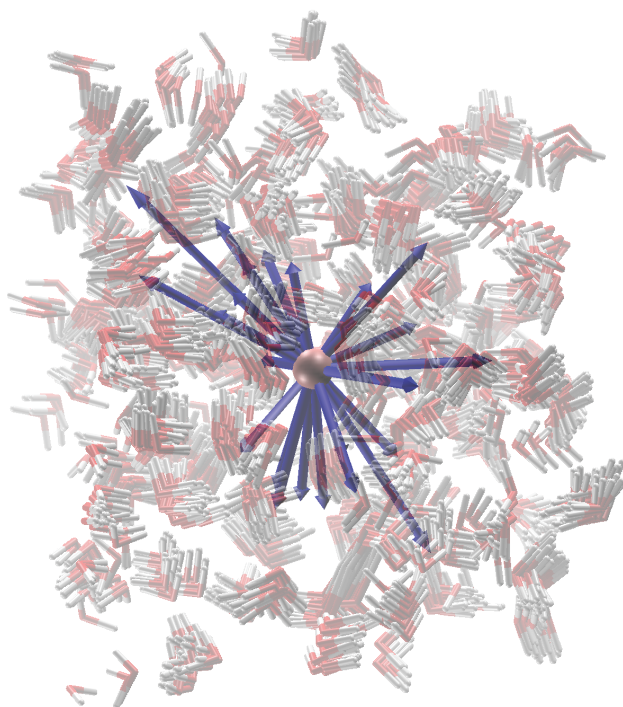


Figure S2: Transition dipole vectors for the CTTS state obtained from TDDFT calculations on 25 snapshots of  $\text{I}^-$ (aq), using the LRC- $\omega$ PBEh(40)-rVV10 functional with a polarizable continuum model.<sup>7,8</sup> The large variability in direction illustrates the substantial microstate dependence in the initial CTTS excitation. The snapshots are superimposed to illustrate the extent of solvent motion across the duration of the trajectory that was sampled.

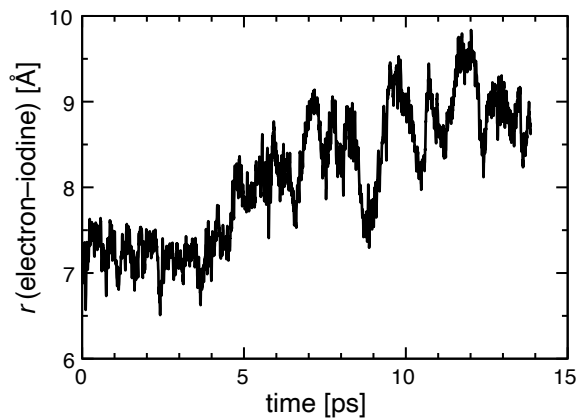


Figure S3: Distance between  $e^-$  (represented by the Wannier center of the SOMO) and  $\text{I}^*$  along the production trajectory of 14 ps, illustrating how the two species diffuse apart.

## References

- [1] Berendsen, H.; Grigera, J.; Straatsma, T. The missing term in effective pair potentials. *J. Phys. Chem.* **1987**, *91*, 6269–6271.
- [2] Kuharski, R. A.; Bader, J. S.; Chandler, D.; Sprik, M.; Klein, M. L.; Imprey, R. W. Molecular model for aqueous ferrous–ferric electron transfer. *J. Chem. Phys.* **1988**, *89*, 3248–3257.
- [3] Straus, J. B.; Calhoun, A.; Voth, G. A. Calculation of solvent free energies for heterogeneous electron transfer at the water–metal interface: Classical versus quantum behavior. *J. Chem. Phys.* **1995**, *102*, 529–539.
- [4] Fulton, J. L.; Schenter, G. K.; Baer, M. D.; Mundy, C. J.; Dang, L. X.; Balasubramanian, M. Probing the hydration structure of polarizable halides: A multiedge XAFS and molecular dynamics study of the iodide anion. *J. Phys. Chem. B* **2010**, *114*, 12926–12937.
- [5] Baer, M. D.; Mundy, C. J. Toward an understanding of the specific ion effect using density functional theory. *J. Phys. Chem. Lett.* **2011**, *2*, 1088–1093.
- [6] Baer, M. D.; Mundy, C. J. An *ab initio* approach to understanding the specific ion effect. *Faraday Discuss.* **2013**, *160*, 89–101.
- [7] Mewes, J.-M.; You, Z.-Q.; Wormit, M.; Kriesche, T.; Herbert, J. M.; Dreuw, A. Experimental benchmark data and systematic evaluation of two *a posteriori*, polarizable-continuum corrections for vertical excitation energies in solution. *J. Phys. Chem. A* **2015**, *119*, 5446–5464.
- [8] Herbert, J. M. Dielectric continuum methods for quantum chemistry. *WIREs Comput. Mol. Sci.* **2021**, *11*, e1519:1–73.